

Newly Designed Quinololinol Inhibitors Mitigate the Effects of Botulinum Neurotoxin A in Enzymatic, Cell-Based and Ex Vivo Assays

Paul T. Bremer, Michael Adler, Cecilia H. Phung, Ajay K. Singh, and Kim D Janda

J. Med. Chem., **Just Accepted Manuscript** • DOI: 10.1021/acs.jmedchem.6b01393 • Publication Date (Web): 14 Dec 2016

Downloaded from <http://pubs.acs.org> on December 14, 2016

Just Accepted

“Just Accepted” manuscripts have been peer-reviewed and accepted for publication. They are posted online prior to technical editing, formatting for publication and author proofing. The American Chemical Society provides “Just Accepted” as a free service to the research community to expedite the dissemination of scientific material as soon as possible after acceptance. “Just Accepted” manuscripts appear in full in PDF format accompanied by an HTML abstract. “Just Accepted” manuscripts have been fully peer reviewed, but should not be considered the official version of record. They are accessible to all readers and citable by the Digital Object Identifier (DOI®). “Just Accepted” is an optional service offered to authors. Therefore, the “Just Accepted” Web site may not include all articles that will be published in the journal. After a manuscript is technically edited and formatted, it will be removed from the “Just Accepted” Web site and published as an ASAP article. Note that technical editing may introduce minor changes to the manuscript text and/or graphics which could affect content, and all legal disclaimers and ethical guidelines that apply to the journal pertain. ACS cannot be held responsible for errors or consequences arising from the use of information contained in these “Just Accepted” manuscripts.

Newly Designed Quinolinol Inhibitors Mitigate the Effects of Botulinum Neurotoxin A in Enzymatic, Cell-Based and *Ex Vivo* Assays

Paul T. Bremer,^a Michael Adler,^b Cecilia H. Phung,^b Ajay K. Singh^b and Kim D. Janda^{a*}

^aDepartments of Chemistry and Immunology, The Skaggs Institute for Chemical Biology, Worm Institute of Research and Medicine (WIRM), The Scripps Research Institute, 10550 North Torrey Pines Road, La Jolla, CA 92037.

^bNeurobehavioral Toxicology Branch, Analytical Toxicology Division, U.S. Army Medical Research Institute of Chemical Defense, 2900 Ricketts Point Road, APG, MD 21010-5400.

Abstract

Botulinum neurotoxin A (BoNT/A) is one of the most deadly toxins, and is the etiological agent of the potentially fatal condition, botulism. Herein, we investigated 8-hydroxyquinoline (quinolin-8-ol) as a potential inhibitor scaffold for preventing the deadly neurochemical effects of the toxin. Quinolinols are known chelators that can disrupt the BoNT/A metalloprotease zinc-containing active site, thus impeding its proteolysis of the endogenous protein substrate, synaptosomal-associated protein 25 (SNAP-25). Using this information, the structure-activity relationship (SAR) of the quinolinol-5-sulfonamide scaffold was explored through preparation of a crude sulfonamide library, and evaluating the library in a BoNT/A LC enzymatic assay. Potency optimization of the sulfonamide hit compounds was undertaken as informed by docking studies, granting a lead compound with a submicromolar K_i . These quinolinol analogues demonstrated inhibitory activity in a cell-based model for SNAP-25 cleavage and an *ex vivo* assay for BoNT/A-mediated muscle paralysis.

Introduction

Clostridium botulinum is a Gram-positive, anaerobic bacterium that naturally biosynthesizes one of the most toxic known substances to mammals, botulinum neurotoxin (BoNT).¹ Although <1 μg of aerosolized toxin is lethal to an adult human,² BoNT also possesses a variety of important medical uses.^{3, 4} of the seven different toxin serotypes (A-G), serotypes A and B are routinely used to treat facial wrinkles,⁵ migraines⁶ and dystonias.⁷⁻

1
2
3
4
5
6
7
8
9
10
11
12
13
14
15
16
17
18
19
20
21
22
23
24
25
26
27
28
29
30
31
32
33
34
35
36
37
38
39
40
41
42
43
44
45
46
47
48
49
50
51
52
53
54
55
56
57
58
59
60

⁹ Unintentional human exposure to BoNT most commonly takes the form of foodborne botulism in adults. The majority of botulism cases in the U.S. were caused by BoNT/A,² which is also the serotype that induces the most severe and persistent symptoms.¹⁰ Indeed, in April of 2015 over 25 people in Ohio were stricken with foodborne BoNT/A, resulting in one patient's death and eleven patients requiring mechanical ventilation.¹¹ The botulism outbreak was the largest in 40 years in the United States, and was caused by improper home canning techniques that failed to kill toxin-producing *C. botulinum* spores.¹¹

Furthermore, BoNT is considered a bioterrorism threat due to its extreme potency; dissemination of BoNT into the air or into a food supply could be devastating to a human population.^{2, 12, 13} The currently approved treatment for botulism is a heptavalent equine antitoxin that is only effective within a limited timeframe.¹⁴

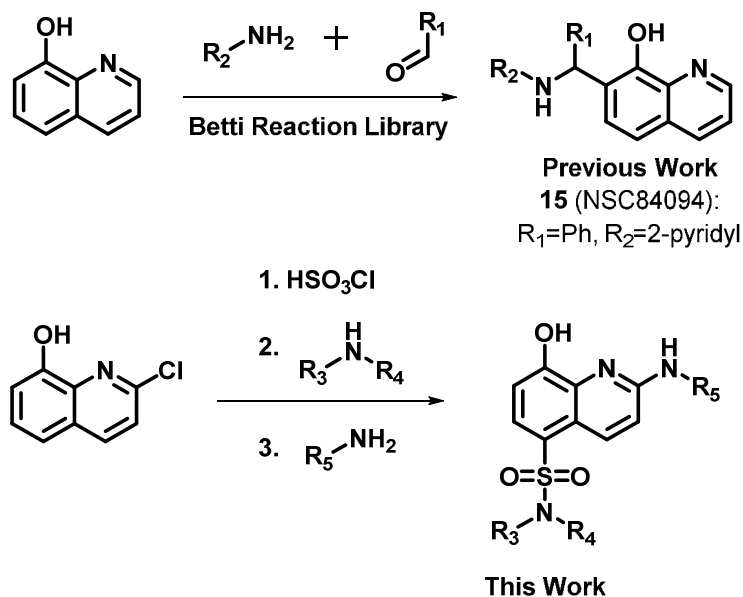
Thus, immunotherapeutic approaches can neutralize the BoNT holotoxin only until the neurotoxin's heavy chain initiates cellular endocytosis.¹⁵ However, following toxin entry into cells, antibodies can no longer prevent the zinc-metalloprotease light chain (LC) of BoNT/A from cleaving its 25 kDa substrate, synaptosomal-associated protein 25 (SNAP-25).¹⁶ Proteolysis of the SNAP-25 protein disrupts fusion of acetylcholine-containing synaptic vesicles with the axon terminal membrane. As a result, muscle fibers no longer receive signals from motor neurons, thus causing muscle paralysis and autonomic dysfunction.¹⁷

Over the past 20 years, a variety of BoNT/A inhibitors have been developed, which target LC endosomal translocation¹⁸⁻²² or the LC protease directly.²³⁻³¹ Zinc-chelating molecules have been shown to be privileged inhibitor scaffolds against zinc metalloproteases e.g. matrix metalloproteinases (MMPs),³²⁻³⁴ for this reason, hydroxamates have been intensely studied as BoNT/A inhibitors.²³⁻²⁵ Despite the numerous disclosures of active site BoNT/A LC inhibitors, rational design of sub-micromolar inhibitors remains challenging. This is due in part to the highly flexible nature of the enzyme, contributing to an induced-fit mechanism that obfuscates prediction of inhibitor binding poses.^{24, 35, 36} An alternative to the hydroxamate, 8-hydroxyquinoline (quinolin-8-ol), has also been found to be a promising BoNT/A LC inhibitor scaffold e.g. compound **15** (NSC84094).²⁸⁻³⁰ The quinolinol core structure is present in the FDA-approved antibiotic chloroxine³⁷ as well as in the experimental drug PBT2, which has been tested in clinical trials as a therapy for Alzheimer's disease.³⁸ A

distinct advantage that quinolinols possess over more traditional zinc-chelating hydroxamates is increased lipophilicity that enhances their ability to penetrate cell membranes, which in effect would increase a molecule's ability to inhibit the intracellular BoNT/A LC.^{29, 30} Previously, the structure-activity relationship (SAR) of the 7-position on the quinolinol ring was explored extensively via screening of a Betti reaction library (Figure 1).²⁸ We hypothesized that functionalization at alternative positions on the quinolinol ring could also be fruitful for the discovery of new and possibly more potent BoNT/A inhibitors.

In our current endeavor, we exploited synthetically facile methods for installing 5-position sulfonamides as well as 2-position amino groups to rapidly identify BoNT/A inhibitor quinolinols (Figure 1). A FRET-based assay for BoNT/A LC substrate cleavage was used for initial inhibitor assessment of our molecules. The most potent leads were tested in a cell assay and *ex vivo* mouse hemidiaphragm assay to determine the therapeutic potential for these molecules to ameliorate the effects of BoNT/A.

Figure 1. Synthetic methods for generating quinolinol libraries



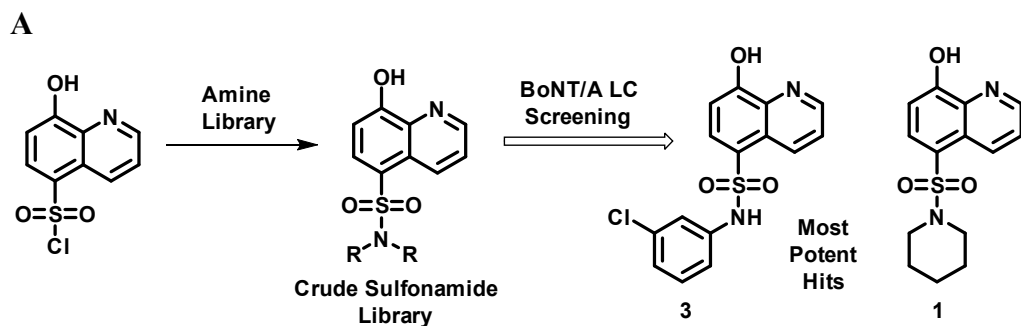
Results and Discussion

Crude Library Screening

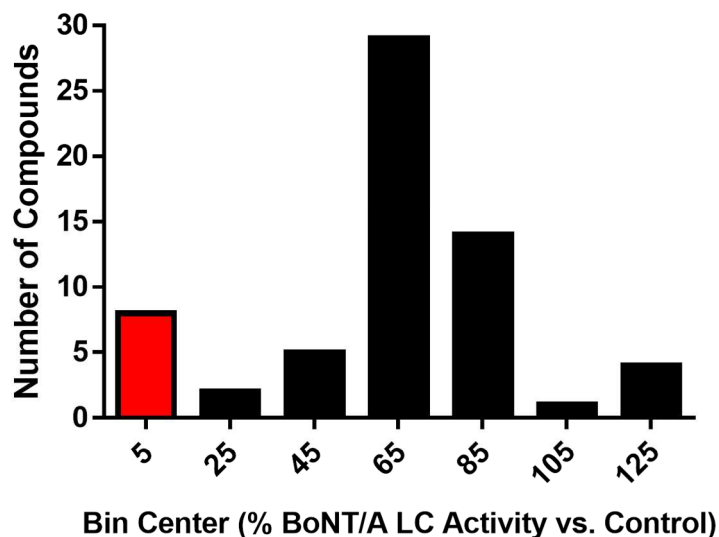
Our primary objective for inhibitor discovery was to identify compounds as efficiently as possible; therefore we sought a simple, yet, high-yielding synthetic methodology to generate molecules without the requirement of

1
2 purification. Given this criterion, we opted to create a sulfonamide library via the reaction of quinolinol-5-
3 sulfonamide with a variety of amine fragments (**Figure 2A**). A total of 63 crude reaction mixtures (**Table**
4 **S1**) at a concentration of $\sim 30 \mu\text{M}$ were screened directly against BoNT/A LC in a FRET-based assay
5 (SNAPTide assay). The majority of the mixtures showed mild inhibition of the LC, and excitingly, 1 in 8 of
6 these crude mixtures reduced enzymatic activity to less than 15% (**Figure 2B**). The eight initial hits were
7 rescreened at a three-fold lower concentration to identify the two most potent compounds (sulfonamides **1** and
8 **3**), which were derived from piperidine and 3-chloroaniline, respectively. It should be noted that the presence of
9 the quinolinol-8-ol moiety did not guarantee BoNT/A LC inhibition as some of the compounds showed little to no
10 activity; and furthermore, quinolinol-8-ol alone does not inhibit the LC. Thus, design and selection of quinolinol
11 aryl ring substituents was essential for achieving potent quinolinol-based inhibitors.

27 **Figure 2. Screening of crude quinolinol-5-sulfonamide library against BoNT/A LC reveals potent**
28 **inhibitors**



B

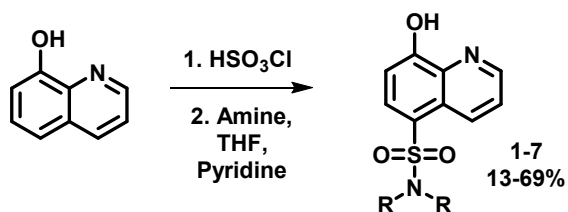


(A) Scheme showing generation of sulfonamide library and structures of hit compounds. (B) Histogram showing distribution of sulfonamide inhibitory activity against BoNT/A LC (relative to DMSO as a control) in the SNAPtide assay. Bin width = $\pm 10\%$ enzyme activity. Compounds were tested at $\sim 30 \mu\text{M}$ and the compounds identified in the red colored bin were rescreened at $\sim 10 \mu\text{M}$ to verify **1** and **3** as hits.

Inhibitor Validation and Preliminary SAR

Through the discovery of **1** and **3** as hit compounds, we were able to demonstrate that the sulfonamide 5-position contributed to BoNT/A LC inhibition. In order to refine inhibitor potency, a series of quinolinol sulfonamides grounded upon **1** and **3** were designed, synthesized and tested (**Figure 3**). When examined in pure form these compounds indeed possessed low μM potency. Analogues of **3** were pursued over **1** because of greater inhibitor potency and availability of a rich source of starting material anilines. Unsubstituted *N*-phenyl sulfonamide **2** showed reduced inhibition, demonstrating the necessity of the 3-chloro substituent. Other functional groups and positions on the phenyl ring were explored in the crude sulfonamide library, but the 3-chloro showed superior inhibitory activity (**Table S1**). Addition of an *N*-methyl substituent increased BoNT/A inhibition as seen with **4** and **5**. Lastly, conformational restriction of the 3-chlorophenyl substituent was explored by introducing 4- and 6-indoline for mimicry of two possible locked rotational conformers; 4-chloroindoline (**7**) displayed markedly better BoNT/A LC inhibition over 6-chloroindoline (**6**) (**Figure 3**).

Figure 3. Synthesis and activity of quinolin-8-ol-5-sulfonamides



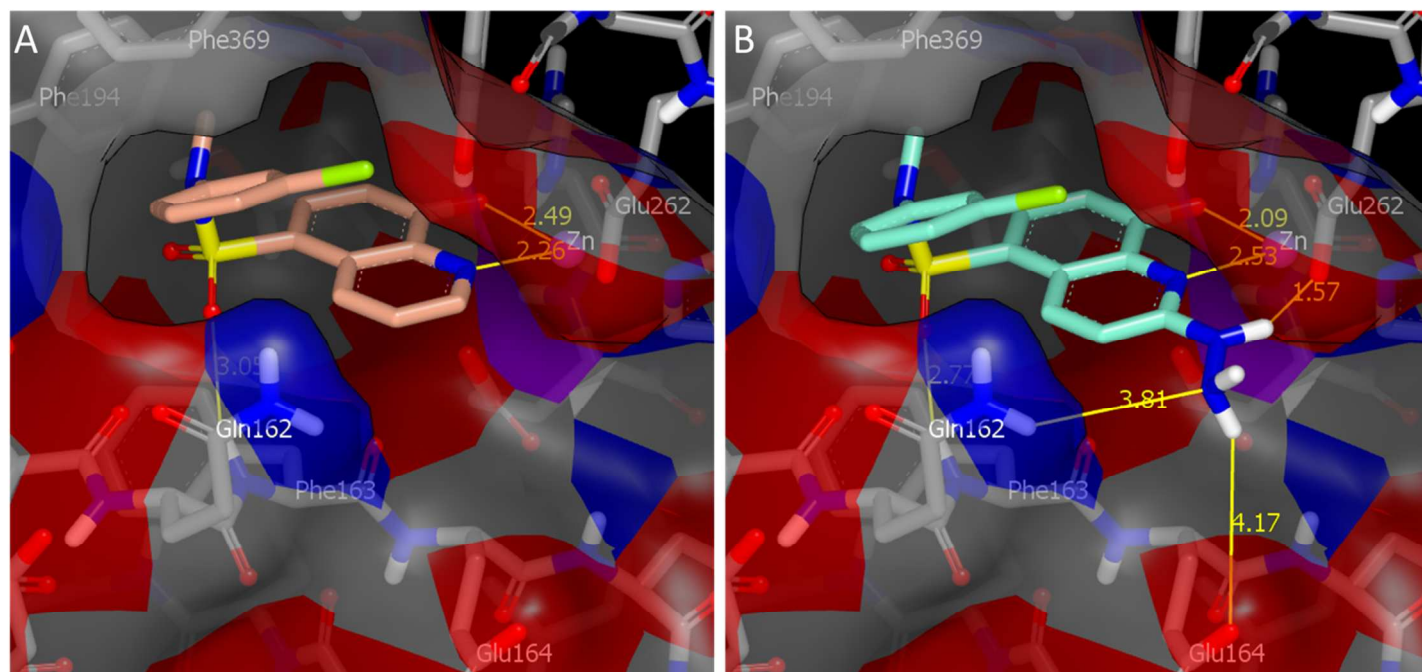
Compound	Amine Used to Prepare Corresponding Sulfonamide	SNAPtide IC_{50} (μM)
1	Piperidine	18.3 ± 5.4
2	Aniline	12.7 ± 0.2
3	3-Chloroaniline	7.32 ± 0.32
4	<i>N</i> -Methylaniline	7.19 ± 0.53
5	<i>N</i> -Methyl-3-Chloroaniline	4.28 ± 0.26

6	6-Chloroindoline	12.8±2.6
7	4-Chloroindoline	3.66±0.08

SAR Optimization Through Docking Studies

In performing SAR optimization on **3**, we arrived at **7** with improved BoNT/A LC inhibition. To achieve further inhibition of the protease, we recruited the insight of computational docking to elucidate positions and functional groups on the quinolinol ring that could garner increased potency. Briefly, lowest energy conformers of **5** were generated using OMEGA³⁹⁻⁴¹ and were docked with FRED⁴²⁻⁴⁴ into the active site which has previously been cocrystalized with hydroxamate inhibitors.²⁵ Because of its zinc-chelating properties, quinolinols, similar to hydroxamates, presumably bind to the BoNT/LC active site zinc.^{29, 30} Docking of **5** into the active site revealed a possible hydrogen bond between the sulfonamide oxygen and a backbone NH of Phe163 in addition to the expected bidentate quinolinol chelation of the zinc. Hydrophobic interactions and/or pi-pi stacking were noted between the chlorophenyl group and Phe369/194. The orientation of compound **5** within the active site suggested that additional interactions with BoNT/A LC could be achieved by functionalizing position 2 or 3 (**Figure 4**). Upon further docking studies, the 2-hydrazino group (**12**) was found to produce favorable fitness scores and appeared to form a hydrogen bond with Glu262. Possible hydrogen bonds were also noted with Glu164 and Gln162, although hydrogen bond lengths were greater than normal.

Figure 1. Docking of compounds **5** and **12** into the BoNT/A LC active site

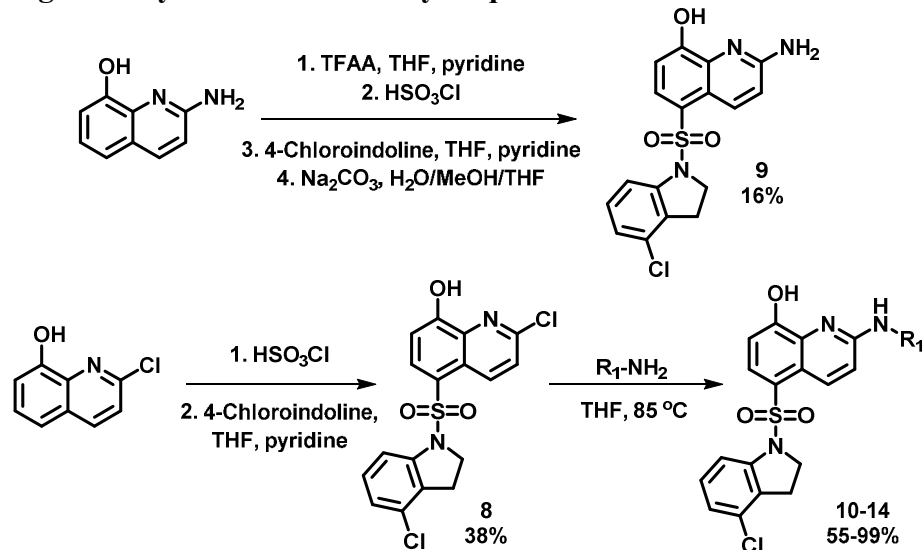


(A) Docking pose of compound **5** shown in tan colored carbons. (B) Docking pose of compound **5** with a 2-hydrazino group added (analogous to compound **12**) shown in light blue colored carbons. Protein receptor carbons are shown in grey with a transparent surface. Relevant residues are labelled and distances between compound-protein metal and possible hydrogen bond interactions are drawn with yellow lines. Receptor crystal structure PDB ID: 4HEV.

In light of this promising docking result, we synthesized a series of 2-aminoquinolinols via an S_NAr reaction with the precursor 2-chloro compound **8** (Figure 5). Poor inhibitory activity of compound **8** was noted with an $IC_{50} > 30 \mu M$, revealing stringency for the 2-position chemotype. Moreover, quinolinols with 2-carboxy or 2-methylamino substituents were inactive, even as the corresponding amides in both cases. In contrast, addition of the 2-amino group in compound **9** presented a similar IC_{50} to the unsubstituted compound **7**, although 2-alkyl amines **10** and **11** showed drastically reduced inhibition, possibly due to repulsion between the lipophilic alkyl groups and polar enzyme amino acid side chains. As we had hoped, a 2.4-fold increase in potency was observed when adding the hydrazino group (**12**) versus the unsubstituted compound **7** (Figure 5). Further modification of the hydrazine with a methyl (**13**) or acetyl (**14**) group slightly decreased inhibitory activity, possibly by interfering with the hydrogen bonding observed in the docking pose (Figure 4). Docking scores showed some correlation with IC_{50} values, and three of the most potent compounds (**5**, **9** and **13**) gave the highest scores (Table S9). Since the quinolinol scaffold is known to inhibit MMPs,³⁴ our most potent compounds were tested

against MMP-1 and -2, revealing inhibitory activity; however, significant selectivity for BoNT/A LC was achieved through addition of 2-hydrazino groups (Table S10).

Figure 2. Synthesis and activity of quinolinol sulfonamides containing a 2-amino substituent



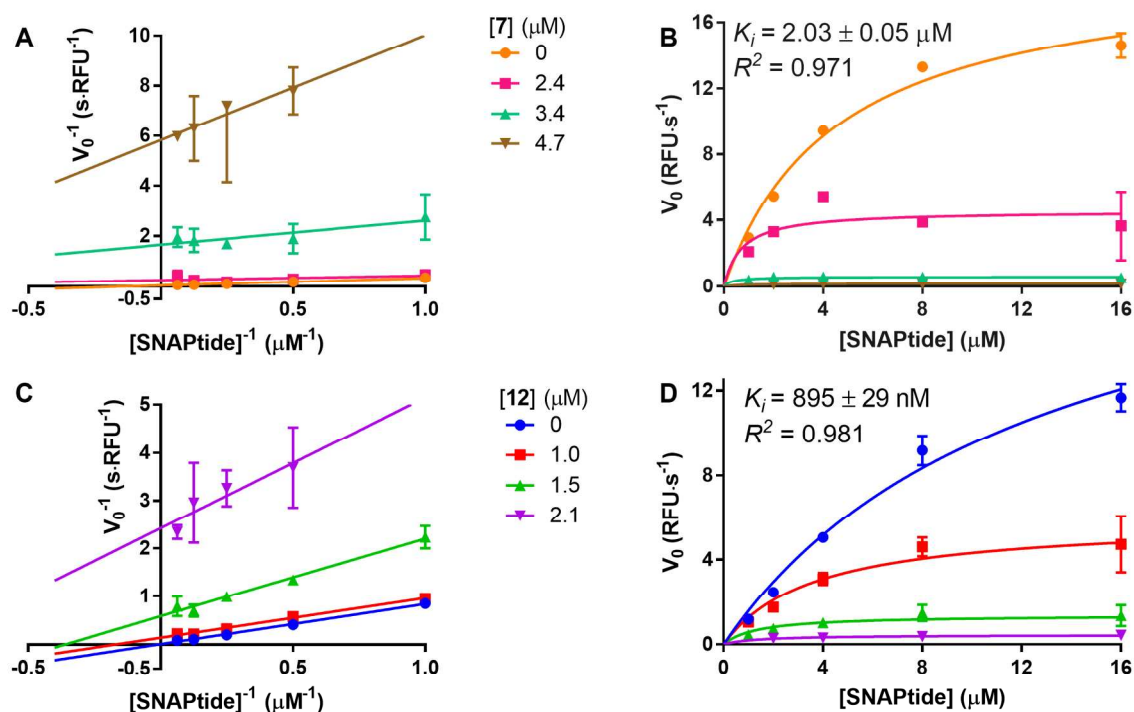
Compound	R ₁	SNAPtide IC ₅₀ (μM)
9	H	3.36±0.09
10	Me	37.6±1.3
11	Et	28.6±4.4
12	NH ₂	1.55±0.05
13	NHMe	3.26±0.01
14	NHAc	5.39±0.15

Quinolinol Sulfonamide Inhibition Kinetics

In considering **12** to be our optimized lead compound, we investigated inhibition kinetics of **12** in the SNAPtide assay along with **7**. Surprisingly, a Lineweaver-Burke plot of the kinetic data suggested an uncompetitive inhibition mechanism for both compounds; with increasing concentrations of inhibitor, both K_m and V_{max} decreased (Figure 6A, 6C). This implies that **7** and **12** bind to the enzyme-substrate (ES) complex, which increases BoNT/A LC affinity for the substrate while inhibiting protease activity. A global fit of this data with an uncompetitive inhibition model revealed a fairly potent, submicromolar K_i of 895 nM for **12** (Figure 6D)

while **7** was less potent as expected (**Figure 6B**). Active site inhibitors of BoNT/A LC such as hydroxamates typically demonstrate competitive inhibition,²⁵ thus the observation of uncompetitive inhibition is unexpected. A notable example of an uncompetitive inhibitor is the natural product brefeldin A; the nature of its inhibition mechanism is attributed to its potent effects on disrupting protein transport from the endoplasmic reticulum.⁴⁵ It is difficult to interpret the biological implications of the uncompetitive mechanism of **7** and **12**, but it could play a role in its activity against BoNT/A (**Figure 8**). Because the compounds presumably bind only to the ES complex, it may exclusively target an active enzyme conformation, possibly leading to their efficacy in advanced BoNT/A models (**Figure 7, 8**). On the other hand, quinolinol uncompetitive inhibition may not occur within BoNT/A-intoxicated cells in the presence of the natural substrate SNAP-25 and could be a kinetic anomaly from the synthetic FRET substrate used in the *in vitro* assay. Overall, the kinetic results neither support nor refute the predicted binding mode in **Figure 4** because uncompetitive inhibitors can bind to either active or allosteric sites.⁴⁶

Figure 3. Inhibition kinetics of compounds 7 and 12 against BoNT/A LC

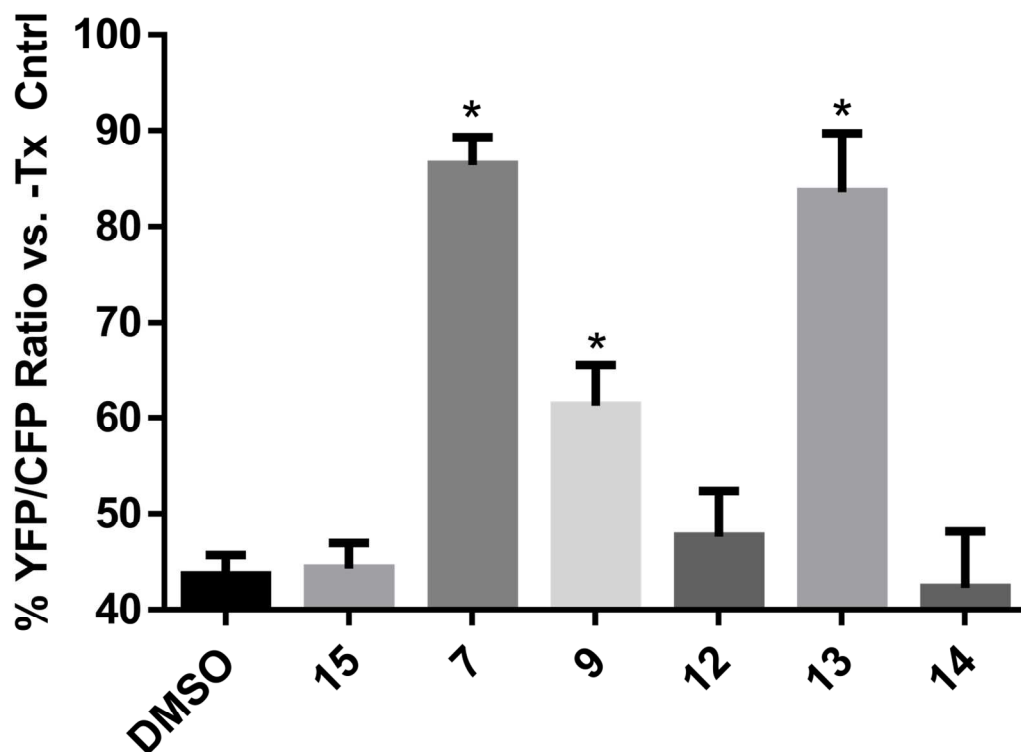


1
2
3 (A) Lineweaver-Burke plot of compound **7** kinetic data. Paralell lines suggest an uncompetitive inhibition
4 mechanism as both K_m and V_{max} are decreasing with increasing [I]. (B) Global fit of compound **7** kinetic data
5 using an uncompetitive inhibition model for K_i determination. (C) Lineweaver-Burke plot of compound **12**
6 kinetic data. (D) Global fit of compound **12** kinetic data (uncompetitive model). All points represent means \pm
7 SEMs. Data were obtained in duplicate in the SNAPtide FRET assay using the fIP6 substrate.
8
9

10 Evaluation of Quinolinol-5-Sulfonamides in Advanced BoNT/A Assays

11
12 Given the promising inhibitory activities of our quinolinols against BoNT/A LC in the enzymatic assay, we
13 investigated these compounds in more advanced biological models for BoNT/A intoxication, which included a
14 cell assay and an *ex vivo* mouse muscle assay. For the cell assay, we employed a specific neuron-like cell line
15 (BoCell) that expresses a recombinant full-length SNAP-25 containing cyan fluorescent protein (CFP) and
16 yellow fluorescent protein (YFP) at the N- and C-termini, respectively. The fusion protein acts as a BoNT/A
17 biosensor for real-time monitoring of SNAP-25 cleavage by the LC protease within live cells resulting in a
18 decreased YFP/CFP ratio.⁴⁷ Treatment of these cells with **7**, **9** and **13** caused a reduction in BoNT/A-mediated
19 proteolysis of the SNAP-25 reporter, as indicated by statistically significant YFP/CFP ratio increases in the
20 presence of the compounds (Figure 7). Compound **13** was the most potent and even showed efficacy at a two-
21 fold lower concentration (Table S11). As a cautionary note, **7** and **13** decreased the YFP/CFP ratio without
22 toxin (Table S11), which could be explained by modest cytotoxicity in XTT and MTT assays (Figure S3, S4);
23 however, this did not obscure their observed efficacy, since +toxin values are normalized to their respective –
24 toxin controls (Figure 7). Compounds **12**, **14** and previously reported quinolinol **15**²⁹ were not active. Although
25 not particularly surprising for **14**, since it showed less inhibition in the SNAPtide assay, lack of cell-based
26 activity for **12** was unexpected. We cannot fully account for the inactivity of **12**, but the presence of an
27 unmodified hydrazino group may result in a reduced cell-membrane permeability or intracellular modification
28 compared to the active, methylated hydrazide **13**. Fortunately, three of our compounds showed noticeably better
29 potency versus a benchmark BoNT/A LC inhibitor **15**,^{28, 29} which had never been examined in the BoCell assay,
30 until now (Figure 7).
31
32
33
34
35
36
37
38
39
40
41
42
43
44
45
46
47
48
49
50
51
52
53
54
55
56
57

58 **Figure 4. Quinolinols inhibit BoNT/A LC-mediated cleavage of SNAP-25 in live cells**
59
60

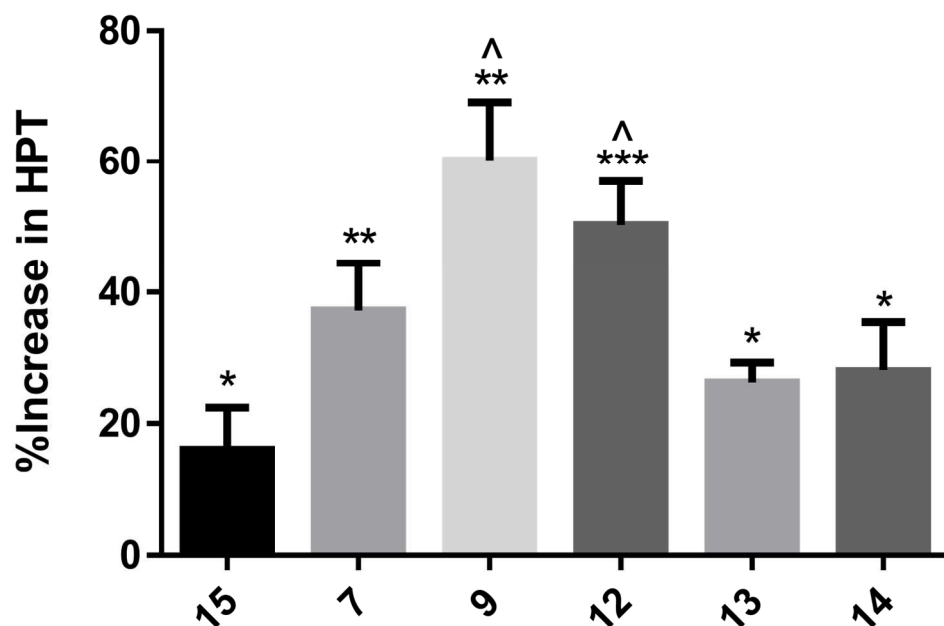


BoCells expressing a recombinant SNAP-25 linked to CFP and YFP at the N- and C-termini, respectively, were exposed to 50 pM BoNT/A (Tx) for 1 h followed by the listed compounds at 25 μ M or DMSO vehicle for 20 h. YFP and CFP fluorescence was then measured and expressed as the YFP/CFP ratio. A decrease in this ratio is indicative of an increase in SNAP-25 cleavage. -Tx controls were included for each compound and +Tx fluorescence ratios were normalized to these controls to produce mean percentage values and SDs over twelve replicates as represented in the figure. * $p < 0.001$ by one-way ANOVA with Dunnett's post-hoc test vs. +Tx DMSO control (left bar).

Lead structures **7**, **9** and **12-14** were further evaluated in a gold-standard *ex vivo* assay for BoNT/A intoxication that consists of electrophysiological monitoring of mouse hemidiaphragm muscles as they succumb to the paralytic effects of the toxin. The assay has been used previously to evaluate a variety of inhibitors including **15**.^{29, 48} Results from our experiments demonstrate that all quinolinols tested, to some degree, extended half-paralysis time (HPT) of BoNT/A-intoxicated mouse hemidiaphragms (**Figure 8**, **Table S12**) with **9** and **12** being the most potent (see **Figure S1** for representative time course of muscle twitch tension). Statistically significant increases in HPT for **9** and **12** were observed compared to **15**, which was the weakest at ameliorating BoNT/A paralysis (**Figure 8**). Although **12** was inactive in the cell assay, its marked activity in the *ex vivo* assay could be attributed to a beneficial, off-target effect in impairing BoNT/A LC endosomal translocation because previous studies have demonstrated that quinolines possess this mechanism of action.^{19, 20}

Demonstration of efficacy in the hemidiaphragm assay is crucial for establishing therapeutic relevance of quinolinols for mitigating BoNT/A. Although the cell-based assay is important for assessing inhibition of BoNT/A LC proteolysis of SNAP-25, the *ex vivo* assay gives a more complete picture of BoNT/A intoxication through measuring diaphragm muscle contraction signaled by the phrenic nerve. The fact that our quinolinols show activity in both assays indicates their potential use for the symptomatic relief of botulism.

Figure 8. Quinolinols mitigate BoNT/A paralysis of mouse hemidiaphragms



Pairs of mouse hemidiaphragms ($n = 4-7$) were treated with the indicated compounds at 20 μM in DMSO or DMSO vehicle for 1 h and then exposed to 5 pM BoNT/A. The time required to achieve 50% twitch tension was noted (half-paralysis time, HPT), and the % increases in HPT for inhibitor-treated hemidiaphragms versus vehicle-treated hemidiaphragms are reported as means and SEMs. The difference between vehicle and compound treated groups was statistically significant ($*p < 0.05$, $**p < 0.01$, $***p < 0.001$) by a paired t-test. Significant differences between compounds were noted by a one-way ANOVA, $F_{5,26} = 5.237$, $p = 0.0019$; $^{\wedge}p < 0.01$ versus **15** (left bar) by Dunnett's post-hoc test.

Conclusion

The inhibitory activity of a series of quinolinol derivatives against BoNT/A LC was explored by screening a crude sulfonamide library, utilizing an LC enzymatic assay for readout. Screening the library revealed a clear SAR centered upon the quinolinol 5-position in which *N*-aryl sulfonamides were the most inhibitory (**Figure 2**). Investigation of these initial hits allowed for potency optimization, which gravitated to a conformationally-

1
2 constrained molecule **7** (**Figure 3**). An *in silico* docking survey of potential poses of **7** inside the BoNT/A LC
3 active site revealed that 2-position substituents could provide additional binding interaction with the enzyme
4
5 (**Figure 4**). Indeed, functionalization of the ring with a 2-hydrazino group (compound **12**) increased potency
6
7 (**Figure 5**). A kinetic evaluation of **12** revealed a submicromolar K_i with an interesting uncompetitive inhibition
8
9 mechanism (**Figure 6**). The most active quinolinols caused BoNT/A LC inhibition in both a cell-based assay
10
11 (**Figure 7**), and an *ex vivo* mouse hemidiaphragm assay (**Figure 8**). Overall, compounds **7**, **9** and **12-14** showed
12
13 greater efficacy in these assays than a previously reported reference compound **15**, demonstrating an improved
14
15 inhibitor design of the new quinolinols. The physiochemical properties of these quinolinols may require further
16
17 optimization for *in vivo* studies, but our current results provide an excellent starting point for development of a
18
19 potential small-molecule BoNT/A therapeutic.
20
21
22
23
24

25 26 Experimental

27
28 **Crude Sulfonamide Library Screening.** In each well of a polypropylene 96-well plate, 75 μmol (3 eq) of each
29
30 amine was added followed by 100 μL of 1:1 DMSO/1,4-dioxane. Quinolin-8-ol-5-sulfonyl chloride (6 mg, 25
31
32 μmol) in 100 μL 1,4-dioxane was then added to each well. The 63 reaction mixtures in the plate were shaken
33
34 for 18 h. Each crude product mixture was diluted 100-fold into DMSO to make an estimated 2.5 mM stock
35
36 solution, which was tested against the BoNT/A LC in the SNAPtide assay at ~ 30 μM for all compounds and
37
38 ~ 10 μM for the hits. For each row on the plate, a DMSO only control well was included as a 100% enzyme
39
40 activity reference, and inhibitor treated wells were normalized to the control. See **Table S1** for identity of
41
42 amines used for library preparation.
43
44
45
46

47
48 **SNAPtide Assay.** In a 96-well, half-area opaque plate, 50X solution of compound in DMSO (1 μL) was
49
50 preincubated for 20 min with 24.5 μL of 56 nM recombinant 425aa BoNT/A LC in 40 mM HEPES + 0.1%
51
52 Triton X-100, pH 7.4 buffer. In the same buffer, 24.5 μL of 6 μM SNAPtide substrate (#521 from List Labs)
53
54 was added to the enzyme+compound solution and the plate was read for 25 min at 490 nm (ex)/523 nm
55
56 (em)/495 nm (cutoff). The linear slopes of the assay readout in RFU/s were used to determine V_0 . Resulting V_0
57
58 values, obtained in duplicate at at least four different inhibitor dilutions, were normalized to the control V_0
59
60

1
2
3 (DMSO-treated well) and curves were fit in GraphPad Prism with the equation $V_0 = \frac{100}{1+10^{(\log(IC_{50})-\log([I]))*Hillslope}}$

4
5 to calculate each IC_{50} . For kinetic experiments, a different SNAPtide substrate with a reduced K_m was used
6
7 (fIP6, #523 from List Labs). Kinetic data were fit in GraphPad Prism with the uncompetitive inhibition model
8
9 with a hillslope of 5 to determine K_i .

10
11
12 **Docking.** The Openeye software suite was used for docking under the use of an academic license. The BoNT/A
13
14 LC receptor files were generated from the active sites of PDB structures 3QIY, 4HEV, 3QIZ, 3QJ0, 2IMB and
15
16 2IMA using the Make Receptor program.⁴⁹ The lowest energy conformers of a set of known quinolinols were
17
18 generated with OMEGA³⁹⁻⁴¹ and were docked into the receptors using FRED with the Chemgauss3 scoring
19
20 function.⁴²⁻⁴⁴ Docking into the 4HEV receptor²⁵ gave the most reasonable compound poses with the most metal
21
22 interaction; therefore 4HEV was selected as the receptor for docking experiments (see **Tables S2-9** for docking
23
24 scores). Figures were generated using the VIDA GUI.⁵⁰

25
26
27
28
29 **Materials for Cell Culture.** BoCell assay medium-2 (BAM-2) and BAM-2 supplement were purchased from
30
31 the BioSentinel Inc., Madison, WI. Glutamax (100X), B-27 (50X), 1X phosphate buffer saline (PBS) and fetal
32
33 bovine serum (FBS) were purchased from Life Technologies Corp., Carlsbad, CA. Eagle's Minimum Essential
34
35 Medium (EMEM) with glutamine and penicillin-streptomycin mixture (100X) were purchased from the
36
37 American Type Culture Collection (ATCC), Manassas, VA. BoNT/A was purchased from Metabionics Inc.,
38
39 Madison, WI. Poly-D-lysine coated 96-well (black/clear) plates were purchased from the Corning Inc., Corning,
40
41 NY.

42
43
44
45 **BoCell Culture.** BoCells are a division arrested genetically modified neuron-like cell-line that expresses full-
46
47 length SNAP-25 with CFP and YFP at the N- and C-terminal residues of SNAP-25, respectively. A frozen vial
48
49 of BoCells ($>2.5 \times 10^6$ cells per vial) was thawed at 37 °C for ~2 min with occasional shaking. Cells were
50
51 transferred from the cryogenic vial to a 15 mL conical tube containing 9 mL of pre-warmed EMEM, mixed
52
53 gently with a 10 mL pipette and centrifuged at 1000 rpm for 6 min. The supernatant was removed and cells
54
55 were re-suspended in EMEM (10.5 mL) with 10% FBS, and 1X penicillin-streptomycin. A 100 μ L suspension
56
57
58
59
60

of cells was dispensed into each well of a 96-well (black–clear) poly-D-lysine coated plate. Cells were grown in a 37 °C humidified cell culture incubator in an atmosphere of 95% air/5% CO₂.

BoCell Assay Method. After 24 h, EMEM was removed and replaced by complete BoCell assay medium-2 (CBAM-2), a proprietary formulation that increases sensitivity of cells to BoNT. CBAM-2 was prepared by adding glutamax, B-27 and BAM-2 supplement to basic BAM-2 media according to the manufacturer's instructions. For evaluating inhibitors, cells were exposed to BoNT/A (50 pM) for 1 h. BoNT/A-containing media was then aspirated and cells were washed once with PBS. The test compounds were dissolved in CBAM-2 at 25 μM and added to cells (quadruplicate wells performed three times) for 20 h. At the end of this incubation period, CBAM-2 media containing test compound was removed and replaced with PBS after an intermediate PBS wash. Fluorescence was measured using a plate reader (Bioteck Synergy H4), and cleavage was quantified by the YFP/CFP emission ratio at 526/470 nm in response to excitation at 500 and 434 nm, respectively. Emissions were recorded sequentially for each fluorescent protein. The principle of the assay is that YFP (and its associated 9-mer SNAP-25 fragment) dissociates following cleavage by BoNT/A LC and subsequently undergoes rapid degradation by the cell. In contrast, CFP (and associated 187-mer truncated SNAP-25) remains membrane bound and is retained by the cell. Thus reduction of the YFP emission signals cleavage of SNAP-25, while CFP emission allows data to be normalized for variations cell density. Statistical analysis was performed in GraphPad Prism version 6.

Hemidiaphragm Assay. Experiments were performed *in vitro* on hemidiaphragm muscles dissected from male CD-1 mice (20-25 g). Mice were housed in AAALAC International accredited facilities with food and water available *ad libitum*. To obtain muscle preparations, the animals were euthanized by an overdose of isoflurane and decapitated. Hemidiaphragms with attached phrenic nerves were dissected, mounted in temperature-controlled tissue baths and immersed in Krebs-Ringer bicarbonate solution at 37 °C (Sigma-Aldrich, St. Louis, MO). The solution was bubbled with a gas mixture of 95% O₂/5% CO₂ and had a pH of 7.3. The phrenic nerve was stimulated with 0.2-msec supramaximal (6 V) pulses at 0.033 Hz using a Grass S88 stimulator (Astro-Med, Inc., West Warwick, RI). Muscle twitches were measured with Grass FT03 isometric force displacement

transducers (Astro-Med), digitized and analyzed off-line with pClamp software (Molecular Devices, Sunnyvale, CA, USA). Resting tensions were maintained at 1.0 g to obtain optimal nerve-evoked tensions. Stock solutions of test compounds were dissolved in DMSO at 10 mM and stored at -20 °C until use. The stock solution was added slowly (30 sec) to the bath to prevent precipitation. The experimental protocol was approved by the Animal Care and Use Committee at the United States Army Medical Research Institute of Chemical Defense and all procedures were conducted in accordance with the principles stated in the Guide for the Care and Use of Laboratory Animals and the Animal Welfare Act of 1966 (P.L. 89-544), as amended.

Compounds were studied at a final inhibitor concentration of 20 μ M. Hemidiaphragm preparations were generally pretreated with test compounds for \geq 1h prior to addition of 5 pM BoNT/A (MetabioLogics, Madison, WI). Control muscles were pretreated for 1 h with 0.2% DMSO prior to challenge with 5 pM BoNT/A. At the concentration tested, some compounds produced a partial inhibition of twitch tension (**9, 12, 13**), which was of similar magnitude and time course for the different inhibitors. Inhibition had an onset time of 3-5 min, and resulted in a reduction in tension of $40.4 \pm 1.5\%$ before reaching steady-state at 45.9 ± 5.1 min. To minimize the effect of muscle to muscle variation, one hemidiaphragm was pretreated with test compound and the contralateral diaphragm muscle from the same mouse received an equivalent volume of DMSO. Half-paralysis time (HPT) was determined as the time required for the twitch tension to fall to 50% of its value just prior to BoNT/A addition. Toxin was added from a 100 nM stock solution which was first diluted to 5 nM (1:20 μ L in Krebs-Ringer bicarbonate solution) just prior to adding to a 20-ml muscle bath. Data were expressed as the percent increase in HPT in the test muscle relative to the HPT in the DMSO-treated muscle. For each compound, four to seven replicates were run, and statistical analysis as described in each figure caption was performed in GraphPad Prism version 6.

General Chemistry. All starting materials and reagents were purchased from Combi-Blocks or Sigma-Aldrich. Organic solvents were anhydrous or distilled prior to use. NMR spectra were recorded on a Bruker 600 MHz instrument and peaks are reported in ppm, using the solvent peak as a chemical shift reference. High resolution mass analysis was performed on an Agilent ESI-TOF-MS system. Analysis of purity was performed by

1
2
3 integrating compound peaks on a 254 nm UV trace recorded on a Agilent LCMS with an Agilent Zorbax
4
5 300SB-C8 4.6 X 50 mm 5 μ m column, flow rate 0.5 mL/min, solvent A: H₂O+0.1% COOH, solvent B:
6
7 MeCN+0.1% COOH, gradient 0-4 min: 5-95% B, 4-7 min: 95% B. All compounds with determined IC₅₀
8
9 values (**1-15**) were \geq 95% pure. Compound **15** was synthesized as previously described.²⁸

10
11 **General Procedure for Sulfonamide Synthesis.** (Adapted from previously reported synthetic methods)^{51, 52} To
12
13 a cooled flask (0 °C) containing 8-hydroxyquinoline (850 mg, 5.9 mmol) was added 2.5 mL chlorosulfonic
14
15 acid. The mixture was stirred for 2 h, allowing to warm to rt and poured into 200 mL iced brine. An extraction
16
17 was performed with 100 mL 1:1 THF/EtOAc, which was dried over MgSO₄ and evaporated to yield the crude
18
19 8-hydroxyquinoline-5-sulfonyl chloride (278 mg, 19%). The sulfonyl chloride (22 mg, 0.09 mmol) was
20
21 dissolved in 2 mL THF and 2 eq pyridine (0.18 mmol) and 1 eq aniline or amine (0.09 mmol) was added. The
22
23 solution was stirred for 18 h, diluted with 10 mL EtOAc and washed once with 1 N HCl followed by saturated
24
25 sodium bicarbonate solution. The organic layer was collected, dried and evaporated to yield the pure
26
27 sulfonamide.
28
29
30
31
32

33 **General Procedure for S_NAr Reaction to 2-Amino-8-hydroxyquinoline-5-sulfonamides.** In a sealed vial, 2-
34
35 chloro-quinolinol compound **8** (10 mg, 26 μ mol) was dissolved in 0.5 mL THF and 50 eq of the desired amine
36
37 or hydrazide. The mixture was stirred at 85 °C for 22 h. Alternatively, the same reaction could be performed
38
39 under 150 W microwave radiation at 150 °C for 22 min in 0.25 mL dioxane. The volatiles were removed under
40
41 high vacuum to afford the crude product which was dissolved in 1 mL 1:1 EtOAc/THF and washed with water
42
43 and saturated sodium bicarbonate solution. The organic layer was dried and evaporated to afford the pure 2-
44
45 amino or hydrazino product as a solid.
46
47
48
49

50 *5-(piperidin-1-ylsulfonyl)quinolin-8-ol (1)*. The title compound was prepared from piperidine using the general
51
52 sulfonamide synthesis procedure as a yellow solid (17.9 mg, 69% yield). ¹H NMR (600 MHz, Acetone-*d*₆) δ
53
54 9.15 (d, *J* = 8.7 Hz, 1H), 8.95 (d, *J* = 2.7 Hz, 1H), 8.17 (d, *J* = 8.2 Hz, 1H), 7.77 (dd, *J* = 8.8, 4.0 Hz, 1H), 7.26
55
56 (d, *J* = 8.2 Hz, 1H), 3.10 – 3.05 (m, 4H), 1.58 – 1.51 (m, 4H), 1.44 – 1.37 (m, 2H). ¹³C NMR (151 MHz,
57
58
59
60

1
2 Acetone-*d*₆) δ 158.31, 149.71, 139.04, 135.20, 133.92, 126.46, 124.40, 123.68, 109.37, 47.09, 26.07, 24.13.

3
4 HRMS (ESI-TOF) *m/z*: [M + H]⁺ Calcd for C₁₄H₁₇N₂O₃S 293.0954; Found 293.0956.

5
6
7 *8-hydroxy-N-phenylquinoline-5-sulfonamide (2)*. The title compound was prepared from aniline using the

8
9 general sulfonamide synthesis procedure as a yellow-green solid (3.6 mg, 13% yield). ¹H NMR (600 MHz,

10
11 Acetone-*d*₆) δ 9.25 (brs, 1H), 9.10 (dd, *J* = 8.7, 1.5 Hz, 1H), 8.92 (dd, *J* = 4.1, 1.5 Hz, 1H), 8.23 (d, *J* = 8.3 Hz,

12
13 1H), 7.72 (dd, *J* = 8.7, 4.1 Hz, 1H), 7.20 – 7.12 (m, 3H), 7.15 – 7.06 (m, 2H), 6.98 (tt, *J* = 7.6, 1.3 Hz, 1H). ¹³C

14
15 NMR (151 MHz, Acetone-*d*₆) δ 158.47, 149.73, 138.99, 138.52, 134.42, 133.91, 129.89, 125.64, 125.50,

16
17 125.20, 124.41, 121.37, 109.16. HRMS (ESI-TOF) *m/z*: [M + H]⁺ Calcd for C₁₅H₁₃N₂O₃S 301.0641; Found

18
19 301.0641.

20
21
22
23 *N-(3-chlorophenyl)-8-hydroxyquinoline-5-sulfonamide (3)* The title compound was prepared from 3-

24
25 chloroaniline using the general sulfonamide synthesis procedure as a yellow-green solid (7.8 mg, 26% yield).

26
27
28 ¹H NMR (600 MHz, Acetone-*d*₆) δ 9.50 (s, 1H), 9.09 (dd, *J* = 8.7, 1.5 Hz, 1H), 8.94 (dd, *J* = 4.2, 1.5 Hz, 1H),

29
30 8.29 (d, *J* = 8.3 Hz, 1H), 7.76 (dd, *J* = 8.8, 4.2 Hz, 1H), 7.23 – 7.14 (m, 3H), 7.06 (ddd, *J* = 8.1, 2.2, 0.9 Hz,

31
32 1H), 7.00 (ddd, *J* = 7.9, 2.1, 0.9 Hz, 1H). ¹³C NMR (151 MHz, Acetone) δ 158.79, 149.89, 140.08, 140.01,

33
34 139.05, 134.95, 134.20, 134.16, 131.48, 125.56, 124.86, 124.63, 120.45, 119.02, 109.25. HRMS (ESI-TOF)

35
36
37 *m/z*: [M + H]⁺ Calcd for C₁₅H₁₂ClN₂O₃S 335.0252; Found 335.0248.

38
39
40 *8-hydroxy-N-methyl-N-phenylquinoline-5-sulfonamide (4)*. The title compound was prepared from *N*-

41
42 methylaniline using the general sulfonamide synthesis procedure as a yellow-green solid (5.3 mg, 19% yield).

43
44
45 ¹H NMR (600 MHz, CDCl₃) δ 8.78 (m, 1H), 8.42 (d, *J* = 8.8 Hz, 1H), 8.17 (d, *J* = 8.0 Hz, 1H), 7.36 – 7.15 (m,

46
47 4H), 7.12 – 6.95 (m, 3H), 3.23 (s, 3H). ¹³C NMR (151 MHz, CDCl₃) δ 156.90, 148.37, 141.34, 137.81, 134.75,

48
49 133.54, 129.02, 127.56, 127.26, 125.70, 123.00, 122.34, 108.21, 38.13. HRMS (ESI-TOF) *m/z*: [M + H]⁺ Calcd

50
51 for C₁₆H₁₅N₂O₃S 315.0798; Found 315.0797.

52
53
54 *N-(3-chlorophenyl)-8-hydroxy-N-methylquinoline-5-sulfonamide (5)*. The title compound was prepared from *N*-

55
56 methyl-3-chloroaniline using the general sulfonamide synthesis procedure as a yellow-green solid (5.1 mg, 16%

57
58 yield). ¹H NMR (600 MHz, CDCl₃) δ 8.78 (dd, *J* = 4.2, 1.5 Hz, 1H), 8.42 (dd, *J* = 8.8, 1.4 Hz, 1H), 8.13 (d, *J* =

59
60

8.3 Hz, 1H), 7.33 (dd, $J = 8.8, 4.2$ Hz, 1H), 7.22 (ddd, $J = 8.1, 2.0, 1.0$ Hz, 1H), 7.20 (d, $J = 8.3$ Hz, 1H), 7.16 (t, $J = 8.0$ Hz, 1H), 7.03 (t, $J = 2.0$ Hz, 1H), 6.99 (ddd, $J = 8.0, 2.1, 1.1$ Hz, 1H), 3.15 (s, 3H). ^{13}C NMR (151 MHz, CDCl_3) δ 157.16, 148.57, 142.66, 137.88, 134.54, 134.50, 133.77, 129.95, 127.71, 127.32, 125.60, 125.45, 123.20, 121.96, 108.28, 38.07. HRMS (ESI-TOF) m/z : $[\text{M} + \text{H}]^+$ Calcd for $\text{C}_{16}\text{H}_{14}\text{ClN}_2\text{O}_3\text{S}$ 349.0408; Found 349.0407.

5-((6-chloroindolin-1-yl)sulfonyl)quinolin-8-ol (**6**). The title compound was prepared from 6-chloroindoline using the general sulfonamide synthesis procedure as an off-white solid (6.2 mg, 19% yield). ^1H NMR (600 MHz, CDCl_3) δ 9.08 (d, $J = 8.8$ Hz, 1H), 8.90 – 8.86 (m, 1H), 8.31 (d, $J = 8.3$ Hz, 1H), 7.67 (s, 1H), 7.63 – 7.56 (m, 1H), 7.25 (d, $J = 8.8$ Hz, 1H), 7.02 – 6.96 (m, 2H), 4.01 (t, $J = 8.5$ Hz, 2H), 2.86 (t, $J = 8.5$ Hz, 2H). ^{13}C NMR (151 MHz, CDCl_3) δ 157.34, 148.71, 143.28, 137.99, 134.14, 133.43, 132.94, 130.25, 125.92, 125.48, 123.89, 123.74, 123.18, 115.64, 108.51, 50.64, 27.61. HRMS (ESI-TOF) m/z : $[\text{M} + \text{H}]^+$ Calcd for $\text{C}_{17}\text{H}_{14}\text{ClN}_2\text{O}_3\text{S}$ 361.0408; Found 361.0408.

5-((4-chloroindolin-1-yl)sulfonyl)quinolin-8-ol (**7**). The title compound was prepared from 4-chloroindoline (0.53 mmol scale) using the general sulfonamide synthesis procedure as a yellow solid (130 mg, 68% yield). ^1H NMR (600 MHz, CDCl_3) δ 9.02 (d, $J = 8.7$ Hz, 1H), 8.84 – 8.80 (m, 1H), 8.25 (d, $J = 8.3$ Hz, 1H), 7.53 (dd, $J = 8.7, 4.1$ Hz, 1H), 7.47 (d, $J = 8.1$ Hz, 1H), 7.17 (d, $J = 8.4$ Hz, 1H), 7.13 (t, $J = 8.0$ Hz, 1H), 6.95 (d, $J = 8.1$ Hz, 1H), 3.99 (t, $J = 8.5$ Hz, 2H), 2.90 (t, $J = 8.4$ Hz, 2H). ^{13}C NMR (151 MHz, CDCl_3) δ 157.42, 148.72, 143.41, 138.07, 134.10, 133.04, 131.08, 130.20, 129.25, 125.51, 123.83, 123.74, 123.22, 113.20, 108.46, 49.77, 27.49. HRMS (ESI-TOF) m/z : $[\text{M} + \text{H}]^+$ Calcd for $\text{C}_{17}\text{H}_{14}\text{ClN}_2\text{O}_3\text{S}$ 361.0408; Found 361.0409.

2-chloro-5-((4-chloroindolin-1-yl)sulfonyl)quinolin-8-ol (**8**). The title compound was prepared in the same manner as compound **7** using 2-chloro-8-hydroxyquinoline as a starting material (115 mg, 0.64 mmol), yielding the product as a yellow solid with a bright pink impurity (97 mg, 38%). ^1H NMR (600 MHz, CDCl_3) δ 8.97 (d, $J = 9.0$ Hz, 1H), 8.20 (d, $J = 8.4$ Hz, 1H), 7.46 (d, $J = 9.0$ Hz, 1H), 7.44 (dd, $J = 8.0, 0.7$ Hz, 1H), 7.20 (d, $J = 8.4$ Hz, 1H), 7.14 – 7.10 (m, 1H), 6.94 (dd, $J = 8.2, 0.8$ Hz, 1H), 3.97 (t, $J = 8.5$ Hz, 2H), 2.89 (t, $J = 8.4$ Hz, 2H). ^{13}C NMR (151 MHz, CDCl_3) δ 156.24, 150.48, 143.12, 137.94, 136.97, 132.74, 131.14, 130.17, 129.26,

1
2
3 124.99, 124.13, 124.00, 123.67, 113.13, 110.17, 49.74, 27.43. HRMS (ESI-TOF) m/z : $[M + H]^+$ Calcd for
4
5 $C_{17}H_{13}Cl_2N_2O_3S$ 395.0018; Found 395.0018.

6
7 *2-amino-5-((4-chloroindolin-1-yl)sulfonyl)quinolin-8-ol* (**9**). To a stirred solution of 2-amino-8-
8
9 hydroxyquinoline (250 mg, 1.56 mmol) and pyridine (1.2 eq, 151 μ L) in 12 mL 1:1 DCM/THF was slowly
10
11 added trifluoroacetic anhydride (1.1 eq, 242 μ L) and the mixture was stirred for 1 h. The volatiles were
12
13 evaporated to produce the crude trifluoroamide-protected intermediate as a grey solid. The solid was suspended
14
15 in 1 mL chloroform and 1 mL chlorosulfonic acid was added. The mixture was stirred for 3 h and poured into
16
17 100 mL iced brine. An extraction was performed with 50 mL 1:1 THF/EtOAc, which was dried over $MgSO_4$
18
19 and evaporated to yield the crude sulfonyl chloride. The sulfonyl chloride (143 mg, 0.40 mmol) was dissolved
20
21 in 5 mL THF and 1.5 eq pyridine (48 μ L, 0.60 mmol) and 1.1 eq 4-chloroindoline (68 mg) was added. The
22
23 solution was stirred for 18 h, diluted with 20 mL EtOAc and washed with 1 N HCl, saturated sodium
24
25 bicarbonate solution and brine. The organic layer was collected, dried and evaporated. The resulting solid was
26
27 dissolved in 2 mL 1:1 THF/MeOH and 2 mL saturated sodium carbonate solution and the mixture was stirred
28
29 for 1 h. The mixture was diluted with water and EtOAc and the organic layer was dried and evaporated to yield
30
31 the pure product as a tan solid (96 mg, 16%). 1H NMR (600 MHz, $DMSO-d_6$) δ 8.47 (d, $J = 9.4$ Hz, 1H), 7.75
32
33 (d, $J = 8.3$ Hz, 1H), 7.28 (dd, $J = 8.2, 0.8$ Hz, 1H), 7.19 (tt, $J = 8.0, 0.8$ Hz, 1H), 7.01 (dd, $J = 8.1, 0.8$ Hz, 1H),
34
35 6.97 (d, $J = 8.3$ Hz, 1H), 6.91 (s, 0H), 6.89 (d, $J = 9.4$ Hz, 1H), 6.75 (s, 2H), 3.97 (t, $J = 8.5$ Hz, 2H), 2.89 (t, $J =$
36
37 8.4 Hz, 2H). ^{13}C NMR (151 MHz, $DMSO-d_6$) δ 156.99, 155.83, 143.29, 137.99, 133.63, 130.32, 129.85,
38
39 129.37, 126.66, 123.09, 121.48, 118.90, 114.52, 112.68, 109.24, 49.57, 26.81. HRMS (ESI-TOF) m/z : $[M + H]^+$
40
41 Calcd for $C_{17}H_{15}ClN_3O_3S$ 376.0517; Found 376.0517.

42
43
44
45
46
47
48
49
50 *5-((4-chloroindolin-1-yl)sulfonyl)-2-(methylamino)quinolin-8-ol* (**10**). The title compound was prepared using
51
52 the general S_NAr procedure using a 2 M methylamine in THF solution. The crude material was purified by silica
53
54 gel preparatory TLC with EtOAc as an eluent to yield the product as a light yellow solid (3.1 mg, 61%). 1H
55
56 NMR (600 MHz, $CDCl_3$) δ 8.61 (d, $J = 9.3$ Hz, 1H), 7.86 (d, $J = 8.3$ Hz, 1H), 7.45 (d, $J = 8.1$ Hz, 1H), 7.12 –
57
58 7.08 (m, 1H), 7.04 (d, $J = 8.3$ Hz, 1H), 6.93 (d, $J = 8.0$ Hz, 1H), 6.68 (d, $J = 9.3$ Hz, 1H), 3.96 (t, $J = 8.5$ Hz,
59
60

2H), 3.07 (d, $J = 4.9$ Hz, 3H), 2.89 (t, $J = 8.5$ Hz, 2H). ^{13}C NMR (151 MHz, CDCl_3) δ 156.09, 155.15, 143.74, 137.76, 134.56, 130.97, 130.26, 129.18, 127.40, 123.61, 123.07, 119.44, 114.26, 113.32, 108.65, 49.67, 29.85, 27.53. HRMS (ESI-TOF) m/z : $[\text{M} + \text{H}]^+$ Calcd for $\text{C}_{18}\text{H}_{17}\text{ClN}_3\text{O}_3\text{S}$ 390.0674; Found 390.0674.

5-((4-chloroindolin-1-yl)sulfonyl)-2-(ethylamino)quinolin-8-ol (**11**). The title compound was prepared using the general $\text{S}_{\text{N}}\text{Ar}$ procedure using a 2 M ethylamine in THF solution yielding the product as a light yellow solid (2.8 mg, 55%). ^1H NMR (600 MHz, CDCl_3) δ 8.61 (d, $J = 9.4$ Hz, 1H), 7.85 (d, $J = 8.3$ Hz, 1H), 7.45 (d, $J = 8.1$ Hz, 1H), 7.12 – 7.08 (m, 1H), 7.03 (d, $J = 8.3$ Hz, 1H), 6.93 (dd, $J = 8.1, 0.8$ Hz, 1H), 6.66 (d, $J = 9.4$ Hz, 1H), 3.96 (t, $J = 8.5$ Hz, 2H), 3.55 – 3.49 (m, 2H), 2.90 (t, $J = 8.5$ Hz, 2H), 1.31 (t, $J = 7.2$ Hz, 3H). ^{13}C NMR (151 MHz, CDCl_3) δ 155.32, 155.01, 143.74, 137.62, 134.61, 130.97, 130.25, 129.18, 127.36, 123.60, 123.06, 119.41, 113.30, 110.13, 108.62, 49.71, 36.53, 27.53, 14.70. HRMS (ESI-TOF) m/z : $[\text{M} + \text{H}]^+$ Calcd for $\text{C}_{19}\text{H}_{19}\text{ClN}_3\text{O}_3\text{S}$ 404.0830; Found 404.0830.

5-((4-chloroindolin-1-yl)sulfonyl)-2-hydrazinylquinolin-8-ol (**12**). The title compound was prepared using the general $\text{S}_{\text{N}}\text{Ar}$ procedure (19 μmol scale) using hydrazine hydrate yielding the product as a brown solid (7.4 mg, 99%). (See **Figure S2** for NMR spectra) ^1H NMR (600 MHz, $\text{DMF-}d_7$) δ 8.59 (d, $J = 9.5$ Hz, 1H), 8.03 (s, 1H), 7.89 (d, $J = 8.3$ Hz, 1H), 7.43 (dd, $J = 8.1, 0.8$ Hz, 1H), 7.25 (tt, $J = 8.1, 0.8$ Hz, 1H), 7.07 (d, $J = 8.3$ Hz, 1H), 7.06 – 7.03 (m, 1H), 7.04 (dd, $J = 8.1, 0.8$ Hz, 1H), 4.10 (t, $J = 8.4$ Hz, 2H), 2.99 (t, $J = 8.4$ Hz, 2H). ^{13}C NMR (151 MHz, $\text{DMF-}d_7$) δ 157.98, 156.69, 144.08, 138.39, 133.37, 130.93, 130.55, 129.63, 127.24, 123.43, 122.68, 119.90, 113.90, 113.23, 109.37, 50.09, 27.34. HRMS (ESI-TOF) m/z : $[\text{M} + \text{H}]^+$ Calcd for $\text{C}_{17}\text{H}_{16}\text{ClN}_4\text{O}_3\text{S}$ 391.0603; Found 391.0304.

5-((4-chloroindolin-1-yl)sulfonyl)-2-(2-methylhydrazinyl)quinolin-8-ol (**13**). The title compound was prepared using the general $\text{S}_{\text{N}}\text{Ar}$ procedure using methylhydrazine yielding the product as a brown solid (5 mg, 99%). ^1H NMR (600 MHz, $\text{Acetone-}d_6$) δ 8.74 (d, $J = 9.6$ Hz, 1H), 7.95 (d, $J = 8.3$ Hz, 1H), 7.44 (dd, $J = 8.1, 0.8$ Hz, 1H), 7.19 (tt, $J = 8.1, 0.9$ Hz, 1H), 7.16 – 7.12 (m, 1H), 7.12 – 7.07 (m, 1H), 6.97 (dd, $J = 8.1, 0.8$ Hz, 1H), 4.06 (t, $J = 8.5$ Hz, 2H), 3.37 (s, 3H), 2.94 (t, $J = 8.5$ Hz, 2H). ^{13}C NMR (151 MHz, $\text{Acetone-}d_6$) δ 157.66, 156.64,

1
2 144.66, 134.89, 131.35, 131.21, 130.03, 128.70, 127.86, 123.95, 123.77, 120.59, 114.17, 113.84, 109.43, 50.50,
3
4 38.68, 27.86. HRMS (ESI-TOF) m/z : $[M + H]^+$ Calcd for $C_{18}H_{18}ClN_4O_3S$ 405.0783; Found 405.0786.

5
6
7 *N'*-(5-((4-chloroindolin-1-yl)sulfonyl)-8-hydroxyquinolin-2-yl)acetohydrazide (**14**). Hydrazide **12** (25 mg, 0.064
8
9 mmol) was dissolved in 400 μ L THF and 1.1 eq acetic anhydride (6.7 μ L, 0.07 mmol) and pyridine (7.7 μ L,
10
11 0.096 mmol) were added. The mixture was stirred for 1 h and then diluted with 400 μ L of MeOH, 400 μ L
12
13 saturated sodium carbonate solution and 400 μ L H_2O . After 30 min of stirring, 500 μ L EtOAc was added and
14
15 the organic layer was washed with sat. sodium bicarbonate solution, collected, dried and evaporated to give the
16
17 product as a yellow-brown solid (22.2 mg, 80%). The product could also be prepared using the general S_NAr
18
19 procedure with acetohydrazide. 1H NMR (600 MHz, Acetone- d_6) δ 8.78 (d, $J = 9.3$ Hz, 1H), 7.97 (d, $J = 8.3$ Hz,
20
21 1H), 7.46 (d, $J = 8.1$ Hz, 1H), 7.20 (m, 1H), 7.19 (t, $J = 8.1$ Hz, 1H), 7.07 (d, $J = 8.4$ Hz, 1H), 6.96 (d, $J = 8.1$
22
23 Hz, 1H), 4.05 (t, $J = 8.4$ Hz, 2H), 2.94 (t, $J = 8.4$ Hz, 2H), 2.07 (s, 3H). ^{13}C NMR (151 MHz, Acetone- d_6) δ
24
25 168.80, 156.61, 156.31, 144.55, 138.00, 135.60, 131.33, 131.20, 129.96, 129.00, 123.96, 123.86, 121.31,
26
27 113.83, 113.36, 109.68, 50.46, 27.83, 26.12. HRMS (ESI-TOF) m/z : $[M + Na]^+$ Calcd for $C_{19}H_{17}ClN_4O_4SNa$
28
29 455.0557; Found 455.0553.
30
31
32
33
34

35 36 Corresponding Author

37
38 *Kim D. Janda email: kdjanda@scripps.edu

39
40 The authors declare no conflict of interest. The views expressed in this article are those of the authors and do
41
42 not reflect the official policy of the Department of the Army, Department of Defense, or the U.S. Government.

43 44 Acknowledgements

45
46 We thank the funding support from NIH grant R01AI119564 (KDJ), The Defense Threat Reduction Agency,
47
48 Joint Science and Technology Office, and Medical S&T Division, award CB4080 (MA). We also acknowledge
49
50 Alex Ducime for synthesis of some inactive quinolinols and Openeye software for use of their docking software
51
52 under an academic license. This is TSRI manuscript # 29418.
53
54
55

56 57 Supporting Information

58
59 The Supporting Information is available free of charge on the ACS Publications website at DOI:
60

1
2
3 Screening library, docking scores and coordinates, selected NMR spectra, MMP assay results, cytotoxicity assay
4 results, representative hemidiaphragm timecourse data and raw data for cell and *ex vivo* assays.
5
6

7 **Author Contributions**

8
9
10 P.T.B. designed, synthesized and tested compounds in the SNAPtide assay, performed docking and wrote the
11 manuscript. M.A. coordinated research at ICD, ran the hemidiaphragm experiments and edited the manuscript.
12
13 C.H.P assisted with the hemidiaphragm experiments including analysis of data. A.K.S. performed the BoCell
14 experiments. K.D.J. was the head research advisor, directed research activities and edited the manuscript.
15
16
17
18

19 **Abbreviations**

20
21 BoNT/A LC, botulinum neurotoxin serotype A light chain; SNAP-25, synaptosomal-associated protein; MMP,
22 matrix metalloproteinase; HPT, half-paralysis time.
23
24
25

26 **References**

- 27
28
29
30 1. Sugiyama, H. Clostridium botulinum neurotoxin. *Microbiol. Rev.* **1980**, *44*, 419-448.
31
32 2. Arnon, S. S.; Schechter, R.; Inglesby, T. V.; Henderson, D. A.; Bartlett, J. G.; Ascher, M. S.; Eitzen, E.;
33 Fine, A. D.; Hauer, J; Layton, M.; Lillibridge, S.; Osterholm, M. T.; O'Toole, T.; Parker, G.; Perl, T. M.;
34 Russell, P. K.; Swerdlow, D. L.; Tonat, K. Botulinum toxin as a biological weapon: Medical and public health
35 management. *J. Am. Med. Assoc.* **2001**, *285*, 1059-1070.
36
37 3. Schantz, E. J.; Johnson, E. A. Properties and use of botulinum toxin and other microbial neurotoxins in
38 medicine. *Microbiol. Rev.* **1992**, *56*, 80-99.
39
40 4. Jankovic, J. Botulinum toxin in clinical practice. *J. Neurol. Neurosurg. Psych.* **2004**, *75*, 951-957.
41
42 5. Fagien, S. Botox for the treatment of dynamic and hyperkinetic facial lines and furrows: Adjunctive use
43 in facial aesthetic surgery. *Plast. Reconstr. Surg.* **1999**, *103*, 701-713.
44
45
46 6. Frampton, J. E. Onabotulinumtoxin A (BOTOX®): A review of its use in the prophylaxis of headaches
47 in adults with chronic migraine. *Drugs* **2012**, *72*, 825-845.
48
49 7. Odergren, T.; Hjaltason, H.; Kaakkola, S.; Solders, G.; Hanko, J.; Fehling, C.; Marttila, R. J.; Lundh, H.;
50 Gedin, S.; Westergren, I.; Richardson, A.; Dott, C.; Cohen, H. A double blind, randomised, parallel group study
51
52
53
54
55
56
57
58
59
60

- 1
2 to investigate the dose equivalence of Dysport (R) and Botox (R) in the treatment of cervical dystonia. *J.*
3
4
5 *Neurol. Neurosurg. Psych.* **1998**, *64*, 6-12.
- 6
7 8. Troung, D. D.; Rontal, M.; Rolnick, M.; Aronson, A. E.; Mistura, K. Double-blind controlled study of
8
9 botulinum toxin in adductor spasmodic dysphonia. *Laryngoscope* **1991**, *101*, 630-634.
- 10
11 9. Roggenkamper, P.; Jost, W. H.; Bihari, K.; Comes, G.; Grafe, S.; Team, N. T. B. S. Efficacy and safety
12
13 of a new botulinum toxin type A free of complexing proteins in the treatment of blepharospasm. *J. Neural*
14
15 *Transm.* **2006**, *113*, 303-312.
- 16
17 10. Woodruff, B. A.; Griffin, P. M.; Mccroskey, L. M.; Smart, J. F.; Wainwright, R. B.; Bryant, R. G.;
18
19 Hutwagner, L. C.; Hatheway, C. L. Clinical and laboratory comparison of botulism from toxin type-A, type-B,
20
21 and type-E in the United States, 1975-1988. *J. Infect. Dis.* **1992**, *166*, 1281-1286.
- 22
23 11. McCarty, C. L.; Angelo, K.; Beer, K. D.; Cibulskas-White, K.; Quinn, K.; de Fijter, S.; Bokanyi, R.;
24
25 Germain, E. S.; Baransi, K.; Barlow, K.; Shafer, G.; Hanna, L.; Spindler, K.; Walz, E.; DiOrio, M.; Jackson, B.
26
27 R.; Luquez, C.; Mahon, B. E.; Basler, C.; Curran, K.; Matanock, A.; Walsh, K.; Slifka, K. J.; Rao, A. K. Large
28
29 outbreak of botulism associated with a church potluck meal - Ohio, 2015. *MMWR Morb. Mortal. Wkly. Rep.*
30
31 **2015**, *64*, 802-803.
- 32
33 12. Wein, L. M.; Liu, Y. F. Analyzing a bioterror attack on the food supply: The case of botulinum toxin in
34
35 milk. *Proc. Natl. Acad. Sci. U.S.A.* **2005**, *102*, 9984-9989.
- 36
37 13. Henderson, D. A. The looming threat of bioterrorism. *Science* **1999**, *283*, 1279-1282.
- 38
39 14. Tacket, C. O.; Shandera, W. X.; Mann, J. M.; Hargrett, N. T.; Blake, P. A. Equine antitoxin use and
40
41 other factors that predict outcome in type-A foodborne botulism. *Amer. J. Med.* **1984**, *76*, 794-798.
- 42
43 15. Simpson, L. I. The binary toxin produced by *Clostridium botulinum* enters cells by receptor-mediated
44
45 endocytosis to exert its pharmacologic effects. *J. Pharmacol. Exp. Ther.* **1989**, *251*, 1223-1228.
- 46
47 16. Blasi, J.; Chapman, E. R.; Link, E.; Binz, T.; Yamasaki, S.; De Camilli, P.; Sudhof, T. C.; Niemann, H.;
48
49 Jahn, R. Botulinum neurotoxin A selectively cleaves the synaptic protein SNAP-25. *Nature* **1993**, *365*, 160-163.
- 50
51
52
53
54
55
56
57
58
59
60

- 1
2
3 17. Schiavo, G.; Rossetto, O.; Tonello, F.; Montecucco, C. Intracellular targets and metalloprotease activity
4 of tetanus and botulism neurotoxins. *Curr. Top. Microbiol. Immunol.* **1995**, *195*, 257-274.
5
6
7 18. Seki, H.; Xue, S.; Pellett, S.; Šilhár, P.; Johnson, E. A.; Janda, K. D. Cellular protection of SNAP-25
8 against botulinum neurotoxin/A: Inhibition of thioredoxin reductase through a suicide substrate mechanism. *J.*
9
10
11
12 *Am. Chem. Soc.* **2016**, *138*, 5568-5575.
13
14 19. Sheridan, R. E.; Deshpande, S. S.; Nicholson, J. D.; Adler, M. Structural features of aminoquinolines
15 necessary for antagonist activity against botulinum neurotoxin. *Toxicon* **1997**, *35*, 1439-1451.
16
17
18 20. Deshpande, S. S.; Sheridan, R. E.; Adler, M. Efficacy of certain quinolines as pharmacological
19 antagonists in botulinum neurotoxin poisoning. *Toxicon* **1997**, *35*, 433-445.
20
21
22
23 21. Kiris, E.; Nuss, J. E.; Stanford, S. M.; Wanner, L. M.; Cazares, L.; Maestre, M. F.; Du, H. T.; Gomba,
24 G. Y.; Burnett, J. C.; Gussio, R.; Bottini, N.; Panchal, R. G.; Kane, C. D.; Tessarollo, L.; Bavari, S. Phosphatase
25 inhibitors function as novel, broad spectrum botulinum neurotoxin antagonists in mouse and human embryonic
26
27
28
29
30
31
32 stem cell-derived motor neuron-based assays. *Plos One* **2015**, *10*.
33
34 22. Kiris, E.; Burnett, J. C.; Nuss, J. E.; Wanner, L. M.; Peyser, B. D.; Du, H. T.; Gomba, G. Y.; Kota, K.
35 P.; Panchal, R. G.; Gussio, R.; Kane, C. D.; Tessarollo, L.; Bavari, S. Src family kinase inhibitors antagonize
36
37
38
39
40
41
42 the toxicity of multiple serotypes of botulinum neurotoxin in human embryonic stem cell-derived motor
43
44
45
46
47
48
49 neurons. *Neurotox. Res.* **2015**, *27*, 384-398.
50
51
52 23. Boldt, G. E.; Kennedy, J. P.; Janda, K. D. Identification of a potent botulinum neurotoxin a protease
53 inhibitor using in situ lead identification chemistry. *Org. Lett.* **2006**, *8*, 1729-1732.
54
55 24. Silvaggi, N. R.; Boldt, G. E.; Hixon, M. S.; Kennedy, J. P.; Tzipori, S.; Janda, K. D.; Allen, K. N.
56 Structures of Clostridium botulinum neurotoxin serotype A light chain complexed with small-molecule
57
58
59
60 inhibitors highlight active-site flexibility. *Chem. Biol.* **2007**, *14*, 533-542.
25. Silhar, P.; Silvaggi, N. R.; Pellett, S.; Capkova, K.; Johnson, E. A.; Allen, K. N.; Janda, K. D.
Evaluation of adamantane hydroxamates as botulinum neurotoxin inhibitors: Synthesis, crystallography,
modeling, kinetic and cellular based studies. *Bioorg. Med. Chem* **2013**, *21*, 1344-1348.

- 1
2
3 26. Kumaran, D.; Rawat, R.; Ludivico, M. L.; Ahmed, S. A.; Swaminathan, S. Structure- and substrate-
4 based inhibitor design for Clostridium botulinum neurotoxin serotype A. *J. Biol. Chem.* **2008**, *283*, 18883-
5 18891.
6
7
8
9
10 27. Silhar, P.; Capkova, K.; Salzameda, N. T.; Barbieri, J. T.; Hixon, M. S.; Janda, K. D. Botulinum
11 neurotoxin A protease: Discovery of natural product exosite inhibitors. *J. Am. Chem. Soc.* **2010**, *132*, 2868.
12
13
14 28. Caglic, D.; Krutein, M. C.; Bompiani, K. M.; Barlow, D. J.; Benoni, G.; Pelletier, J. C.; Reitz, A. B.;
15 Lairson, L. L.; Houseknecht, K. L.; Smith, G. R.; Dickerson, T. J. Identification of clinically viable quinolinol
16 inhibitors of botulinum neurotoxin A light chain. *J. Med. Chem.* **2014**, *57*, 669-676.
17
18
19 29. Roxas-Duncan, V.; Enyedy, I.; Montgomery, V. A.; Eccard, V. S.; Carrington, M. A.; Lai, H. G.; Gul,
20 N.; Yang, D. C. H.; Smith, L. A. Identification and biochemical characterization of small-molecule inhibitors of
21 Clostridium botulinum neurotoxin serotype A. *Antimicrob. Agents Chemother.* **2009**, *53*, 3478-3486.
22
23
24 30. Lai, H. G.; Feng, M. H.; Roxas-Duncan, V.; Dakshanamurthy, S.; Smith, L. A.; Yang, D. C. H.
25 Quinolinol and peptide inhibitors of zinc protease in botulinum neurotoxin A: Effects of zinc ion and peptides
26 on inhibition. *Arch. Biochem. Biophys.* **2009**, *491*, 75-84.
27
28
29 31. Videnovic, M.; Opsenica, D. M.; Burnett, J. C.; Gomba, L.; Nuss, J. E.; Selakovic, Z.; Konstantinovic,
30 J.; Krstic, M.; Segan, S.; Zlatovic, M.; Sciotti, R. J.; Bavari, S.; Solaja, B. A. Second generation steroidal 4-
31 aminoquinolines are potent, dual-target inhibitors of the botulinum neurotoxin serotype A metalloprotease and
32 *P. falciparum* malaria. *J. Med. Chem.* **2014**, *57*, 4134-4153.
33
34
35 32. Jacobsen, F. E.; Lewis, J. A.; Cohen, S. M. A new role for old ligands: Discerning chelators for zinc
36 metalloproteinases. *J. Am. Chem. Soc.* **2006**, *128*, 3156-3157.
37
38
39 33. Puerta, D. T.; Lewis, J. A.; Cohen, S. M. New beginnings for matrix metalloproteinase inhibitors:
40 Identification of high-affinity zinc-binding groups. *J. Am. Chem. Soc.* **2004**, *126*, 8388-8389.
41
42
43 34. Jacobsen, J. A.; Fullagar, J. L.; Miller, M. T.; Cohen, S. M. Identifying chelators for metalloprotein
44 inhibitors using a fragment-based approach. *J. Med. Chem.* **2011**, *54*, 591-602.
45
46
47
48
49
50
51
52
53
54
55
56
57
58
59
60

- 1
2
3 35. Zuniga, J. E.; Schmidt, J. J.; Fenn, T.; Burnett, J. C.; Arac, D.; Gussio, R.; Stafford, R. G.; Badie, S. S.;
4
5 Bavari, S.; Brunger, A. T. A potent peptidomimetic inhibitor of botulinum neurotoxin serotype A has a very
6
7 different conformation than SNAP-25 substrate. *Structure* **2008**, *16*, 1588-1597.
8
9
10 36. Silhar, P.; Lardy, M. A.; Hixon, M. S.; Shoemaker, C. B.; Barbieri, J. T.; Struss, A. K.; Lively, J. M.;
11
12 Javor, S.; Janda, K. D. C-terminus of botulinum A protease has profound and unanticipated kinetic
13
14 consequences upon the catalytic cleft. *ACS Med. Chem. Lett.* **2013**, *4*, 283-287.
15
16
17 37. Rubbo, S. D.; Albert, A.; Gibson, M. I. The influence of chemical constitution on antibacterial activity.
18
19 Part 5: The antibacterial action of 8-hydroxyquinoline (oxine). *Br. J. Exp. Pathol.* **1950**, *31*, 425-441.
20
21
22 38. Cherny, R. A.; Atwood, C. S.; Xilinas, M. E.; Gray, D. N.; Jones, W. D.; McLean, C. A.; Barnham, K.
23
24 J.; Volitakis, I.; Fraser, F. W.; Kim, Y. S.; Huang, X. D.; Goldstein, L. E.; Moir, R. D.; Lim, J. T.; Beyreuther,
25
26 K.; Zheng, H.; Tanzi, R. E.; Masters, C. L.; Bush, A. I. Treatment with a copper-zinc chelator markedly and
27
28 rapidly inhibits beta-amyloid accumulation in Alzheimer's disease transgenic mice. *Neuron* **2001**, *30*, 665-676.
29
30
31 39. OMEGA version 2.4.6. OpenEye Scientific Software, Santa Fe, NM. <http://www.eyesopen.com>
32
33
34 40. Hawkins, P. C. D.; Nicholls, A. Conformer Generation with OMEGA: Learning from the data set and
35
36 the analysis of failures. *J. Chem. Inf. Model.* **2012**, *52*, 2919-2936.
37
38
39 41. Hawkins, P. C. D.; Skillman, A. G.; Warren, G. L.; Ellingson, B. A.; Stahl, M. T. Conformer generation
40
41 with OMEGA: Algorithm and validation using high quality structures from the Protein Databank and
42
43 Cambridge Structural Database. *J. Chem. Inf. Model.* **2010**, *50*, 572-584.
44
45
46 42. FRED version 2.2.5. OpenEye Scientific Software, Santa Fe, NM. <http://www.eyesopen.com>
47
48
49 43. McGann, M. FRED pose prediction and virtual screening accuracy. *J. Chem. Inf. Model.* **2011**, *51*, 578-
50
51 596.
52
53 44. McGann, M. FRED and HYBRID docking performance on standardized datasets. *J. Comput. Aided*
54
55 *Mol. Des.* **2012**, *26*, 897-906.
56
57
58 45. Chardin, P.; McCormick, F. Brefeldin A: The advantage of being uncompetitive. *Cell* **1999**, *97*, 153-
59
60 155.

- 1
2
3 46. Lin, C. W.; Sie, H. G.; Fishman, W. H. L-tryptophan. A non-allosteric organ-specific uncompetitive
4 inhibitor of human placental alkaline phosphatase. *Biochem. J.* **1971**, *124*, 509-516.
5
6
7 47. Min, D.; Tepp, W. H.; Johnson, E. A.; Chapman, E. R. Using fluorescent sensors to detect botulinum
8 neurotoxin activity in vitro and in living cells. *Proc. Natl. Acad. Sci. U.S.A.* **2004**, *101*, 14701-14706.
9
10
11 48. Adler, M.; Dinterman, R. E.; Wannemacher, R. W. Protection by the heavy metal chelator N,N,N',N'-
12 tetrakis (2-pyridylmethyl)ethylenediamine (TPEN) against the lethal action of botulinum neurotoxin A and B.
13
14
15
16
17 *Toxicon* **1997**, *35*, 1089-1100.
18
19 49. Make Receptor version 3.0.1. OpenEye Scientific Software, Santa Fe, NM. <http://www.eyesopen.com>
20
21 50. VIDA version 4.3.0.4. OpenEye Scientific Software, Santa Fe, NM. <http://www.eyesopen.com>
22
23 51. Pearce, D. A.; Jotterand, N.; Carrico, I. S.; Imperiali, B. Derivatives of 8-hydroxy-2-methylquinoline are
24 powerful prototypes for zinc sensors in biological systems. *J. Am. Chem. Soc.* **2001**, *123*, 5160-5161.
25
26
27
28 52. Ariyasu, S.; Sawa, A.; Morita, A.; Hanaya, K.; Hoshi, M.; Takahashi, I.; Wang, B.; Aoki, S. Design and
29 synthesis of 8-hydroxyquinoline-based radioprotective agents. *Bioorg. Med. Chem* **2014**, *22*, 3891-3905.
30
31
32
33
34
35
36
37
38
39
40
41
42
43
44
45
46
47
48
49
50
51
52
53
54
55
56
57
58
59
60

1
2
3
4
5
6
7
8
9
10
11
12
13
14
15
16
17
18
19
20
21
22
23
24
25
26
27
28
29
30
31
32
33
34
35
36
37
38
39
40
41
42
43
44
45
46
47
48
49
50
51
52
53
54
55
56
57
58
59
60

TOC Graphic

